JOURNAL OF MATERIALS SCIENCE 28 (1993) 5560–5568

Microstructure and mechanical properties of isotactic polypropylene (iPP)/polyamide 12 (PA12) blends

J. VARLET
GEMPPM, INSA, 69621 Villeurbanne cedex, France
J. PÉREZ, R. VASSOILLE, G. VIGIER, M. GLOTIN
CERDATOCHEM, 27470 Serquigny, France
J. Y. CAVAILLÉ*
C.E.R.M.A.V.–C.N.R.S., BP 53 X, 38041 Grenoble cedex, France

The microstructure and mechanical properties of polyamide 12/isotactic polypropylene blends with different compositions are studied. It is shown that the injection moulding technique used to process all samples results in a more or less pronounced orientation of macromolecular chains, which in its turn is responsible for a preferential orientation of polymer crystals. At a larger scale, the injection technique is also responsible for the deformation of polyamide domains into ellipsoides when polypropylene is dominant. In contrast, when polyamide is dominant, domains of both polymers are co-continuous in the materials. This feature is discussed on the basis of dynamic mechanical measurements.

1. Introduction

During the last few years, the fields of application of polymer blends has increased more and more. In particular cases, specific physical characteristics such as impact properties or solvent barrier properties are of main interest. For example, it is well known that impact properties are improved by the addition of soft elastomeric inclusions.

In the general search to improve the technological properties of polymers, the main advantage of blending already produced polymers is its reduced cost in comparison with redesigning a complete line of production of new polymers.

A third component, hereafter called "TC", is used to stabilize the blend and to increase interfacial adhesion between homopolymers, thus improving its mechanical properties. In this paper we establish relationships between its macroscopic properties, such as its tensile behaviour and more precisely its elongation after breaking, and its microstructural features, such as the morphology of homopolymer domains or the crystalline orientations.

2. Experimental procedure

2.1. Materials

The selected materials were isotactic polypropylene (iPP)/polyamide 12 (PA12) blends obtained by the injection moulding technique. Samples were provided by Atochem (27470-Serquigny, France). Their number-average molecular weight and their weight-average molecular weight were respectively 25 000 and 47 000 for PA12 and 55 000 and 270 000 for iPP. A third polymer (TC) is blended with iPP and PA12 in order to improve interfacial adhesion. It is a grafted copolymer based on iPP. The material sheets had been moulded into a parallelepipedic plate (70 × 100 × 2 mm) injected from a cylindrical gate.

Therefore, during the operation of filling up, the molten polymer flowed along straight lines from the gate to the far end of the mould under a pressure of 1×10^3 Pa and at a temperature of 220 °C.

Two sets of blends were considered: blends with more iPP than PA12 (iPP/PA 12 = 70/30 vol%), hereafter called "direct blends" (D) their TC content was 1%, 2%, 3% or 10% in weight and corresponding blends were respectively referred to as D1–D10; a blend with more PA12 than (iPP/PA12 = 43/57 vol%) and a TC content of 2 wt%, hereafter named "inverse blend" (I).

2.2. Characterization methods

Four main techniques were used to characterize the blends: wide angle X-ray scattering (WAXS) to characterize crystal lattices, small angle X-ray scattering (SAXS) to characterize the crystalline domains and mechanical spectrometry and scanning electron microscopy to characterize homopolymer domains.

2.2.1. X-ray scattering

Measurements were performed by transmission in order to have information from the core to the skin of

---

* Author to whom correspondence should be addressed.

the samples. The same apparatus was used for WAXS and SAXS. It includes a Rigaku X-ray generator producing CuK_α radiation, a collimation system including perpendicular mirrors and a linear detector of 512 channels, each of them of 104 μm. When the detector is closer than 0.1 m to the sample, measurements lead to wide angle results ($5° < \theta < 15°$). When the distance from the sample is 3 m, measurements lead to small angle results $0.3° < \theta < 1.15°$.

Three sets of measurements were made in such conditions that the X-ray beam was aligned along the three principle directions, x, y, z of the sheet (Fig. 1), where Y is the injection direction. For each direction of the incident beam, the transmitted beam was collected in three distinct directions of the detector, corresponding to successive $\pi/4$ rotations around the incident beam axis (Fig. 1). For example, a beam aligned along the X axis leads to three different patterns referred to as D_x^0, D_x^{45} and D_x^{90}, where D_x^0 corresponds to a direction perpendicular to the injection axis. A beam aligned along the z axis leads to patterns referred to as D_z^0, D_z^{45} and D_z^{90} where D_z^0 also corresponds to a direction perpendicular to the injection axis. A beam aligned along the y axis leads to patterns referred to as D_y^0, D_y^{45} and D_y^{90}, where D_y^0 corresponds to a direction parallel to the surface of the sheet.

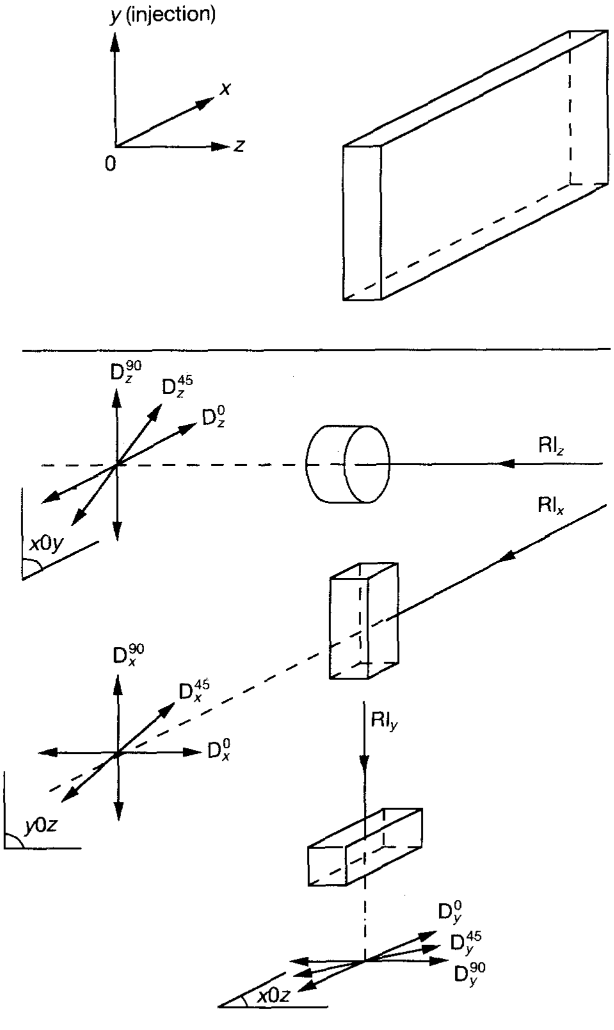

Figure 1 Relative orientation of X-ray beam, sample and detector for WAXS and SAXS experiments.

2.2.2. *Scanning electron microscopy*

Observation surfaces were prepared by two different methods, (i) fracture at low temperature, in liquid nitrogen and (ii) cutting with a microtome at low temperature, in liquid nitrogen. In the first case, the contrast is due to the topology of the fractured surfaces. In the second case, the contrast is improved (i) for the blends, by extracting PA12 with a specific solvent (hexa-fluoro-isopropanol) at room temperature and (ii) for pure iPP, by etching with a 6 g l^{-1} solution of orthophosphoric acid (1 volume) and sulphuric acid (1 volume) [1].

All samples were gold metallized to obtain a superficial conduction.

2.2.3. *Mechanical spectrometry*

2.2.3.1. Experimental procedure. The shear dynamic modulus $G^* = G' + iG''$ was measured by means of a mechanical spectrometer working in the frequency range 10^{-5}–5 Hz and temperature range 100–700 K (Micromecanalyser, Metravib Instruments, France). The maximum strain was lower than 10^{-4}, ensuring that stress and strain were linear for all experiments.

2.2.3.2. Methodology. It is noteworthy that the mechanical behaviour of a multiphase system depends mainly upon two sets of parameters [2], namely the geometrical arrangement of phases, i.e. the morphology of homopolymer domains, and the behaviour of each phase.

The adhesion is supposed to be perfect for the very low deformations required by this method. Using a model for composite systems, it is then possible to predict the behaviour of the blend from (1) knowledge of the behaviour of the homopolymers and (2) some hypothesis on their respective topological arrangement [3]. Reasons for differences between calculated data and experimental data of the blend are of two types, namely (i) the hypothesis on geometrical and topological arrangement of domains are to be modified, and (ii) mechanical relaxations of the bulk homopolymers are different when these homopolymers are included in the blend. It is noteworthy that the presence of TC can also modify the behaviour of the components. Thus it appears that information can be obtained from a comparison between experimental and calculated data. All measurements were made at a frequency of 0.1 Hz in the temperature range 100–450 K. The temperature step between two subsequent measurements is 2K.

In order to calculate the complex shear modulus of the blend as a function of temperature, data for pure homopolymers were combined for each temperature. Before measurements, samples were submitted to an *in situ* annealing at 140 °C (413 K) for 90 min. We have recently shown [4] that under these conditions the incidence of absorbed water on mechanical relaxations of PA12 is avoided: liquid nitrogen which is around the enclosure permits the trapping of water molecules and leads to very efficient drying.

3. Mechanical properties

3.1. Experimental procedure

Tensile tests were conducted to investigate mechanical properties. Samples were bars of dumbell form, of length 30 mm and with a rectangular section 4×2 mm in size. Bars were cut by means of a laser beam: the laser beam emitted by a CO_2 source is focussed to obtain a light concentration of 10^6 W cm^{-2}. It leads to a superficial melting of polymers which avoids the occurrence of defects on the surface of the samples. These bars were submitted to a tensile force in an Instron apparatus, with a stress cell allowing measurements up to 10^5 N. The relative elongation at break of the bars, referred to as λ_R, was measured. Two sets of bars were prepared for each system, bulk homopolymers and blends, (i) bars with their axes along the injection direction ($\|$), and (ii) bars with their axis perpendicular to the injection direction ($\perp$).

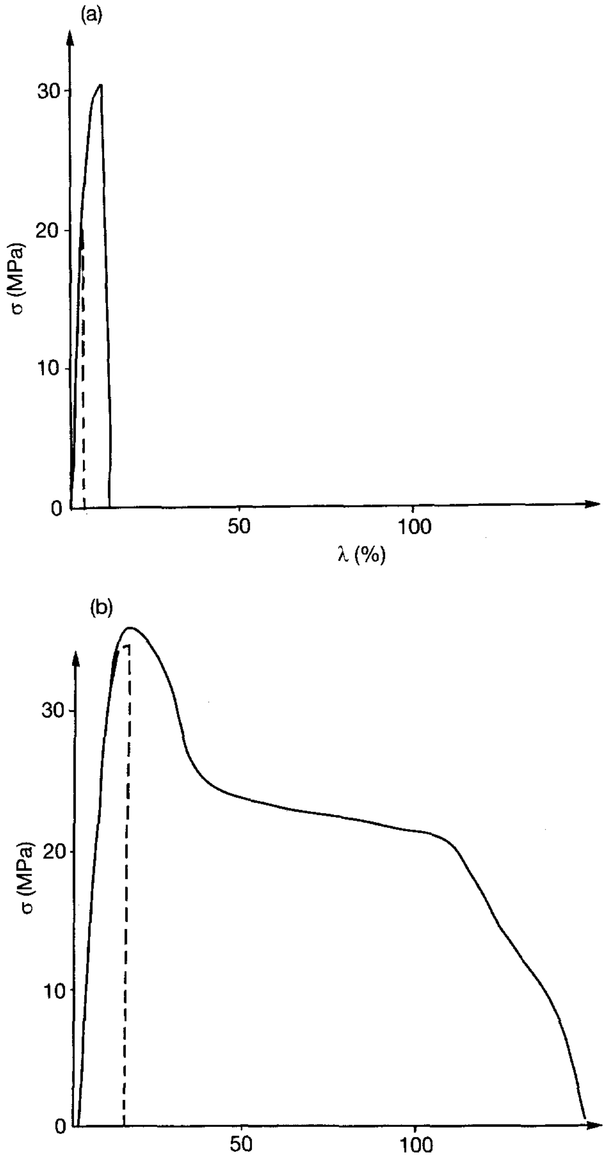

Figure 2 Curves of applied stress versus relative elongation for blends (a) D1 and (b) D10. Full line corresponds to samples oriented along the injection direction. Dotted line corresponds to samples oriented perpendicular to the injection direction.

TABLE I

	$\lambda_R\|$ (%)	$\lambda_R\perp$ (%)	$\sigma_R\|$ (MPa)	$\sigma_R\perp$ (MPa)
Homopolymers				
iPP	60	28	31	30
PA12	244	287	35.5	37
Blends				
D1	12	4.5	32.5	19.5
D2	12.5	6	32.5	19
D3	16.5	6.5	33.5	23.5
D10	106	10	37	29
I	8	1.9	33.3	13.6

3.2. Results

The curves of stress versus relative elongation are presented in Fig. 2 for blends D1 and D10 and for each direction (parallel and perpendicular to the injection direction). In both cases, it appears that the elongation at break is much higher for samples cut along the injection direction; we will call this particularity a mechanical anisotropy. In addition, the presence of TC seems to increase the elongation at break. Results for homopolymers and blends are reported in Table I. It includes the values of λ_R and stress at break σ_R for each direction, referred to as ($\|$) and ($\perp$).

These results lead us to three main conclusions: the influence of TC on the break behaviour is confirmed; a mechanical anisotropy arises in all systems, nevertheless, it is lower for pure homopolymers and almost nonexistent for PA12; the blend I shows a particular behaviour, values of λ_R are much smaller than for blends D in each direction.

4. Interpretation of microstructural features

Our aim is to obtain information at different levels of microstructure so as to understand the mechanical properties of blends, as shown in part 2. We will now describe the results obtained by the different characterization methods.

A final discussion will give precise relationships between microstructure and mechanical behaviour.

4.1. Crystalline orientation

Pure iPP was first studied by means of X-ray scattering and SEM. Fig. 3 shows the diffraction patterns obtained for each direction of the incident beam, in the case of pure iPP. Dependence of diffraction patterns on the incident direction suggests that pure iPP shows a strong crystalline orientation.

Variations around both the x and z axes are similar: D_x^0, D_x^{45} and D_x^{90} are similar to D_z^0, D_z^{45} and D_z^{90}, respectively. In contrast, D_y^θ seems to be independent of θ for $\theta = 0$, 45 and 90°. Thus we conclude that the average orientation of the crystal lattice is isotropic around the y axis.

The reflexion peaks of Fig. 3 were associated with lattice planes (h k l), according to NATTA's data [5], for the α-crystalline form of iPP which is known to

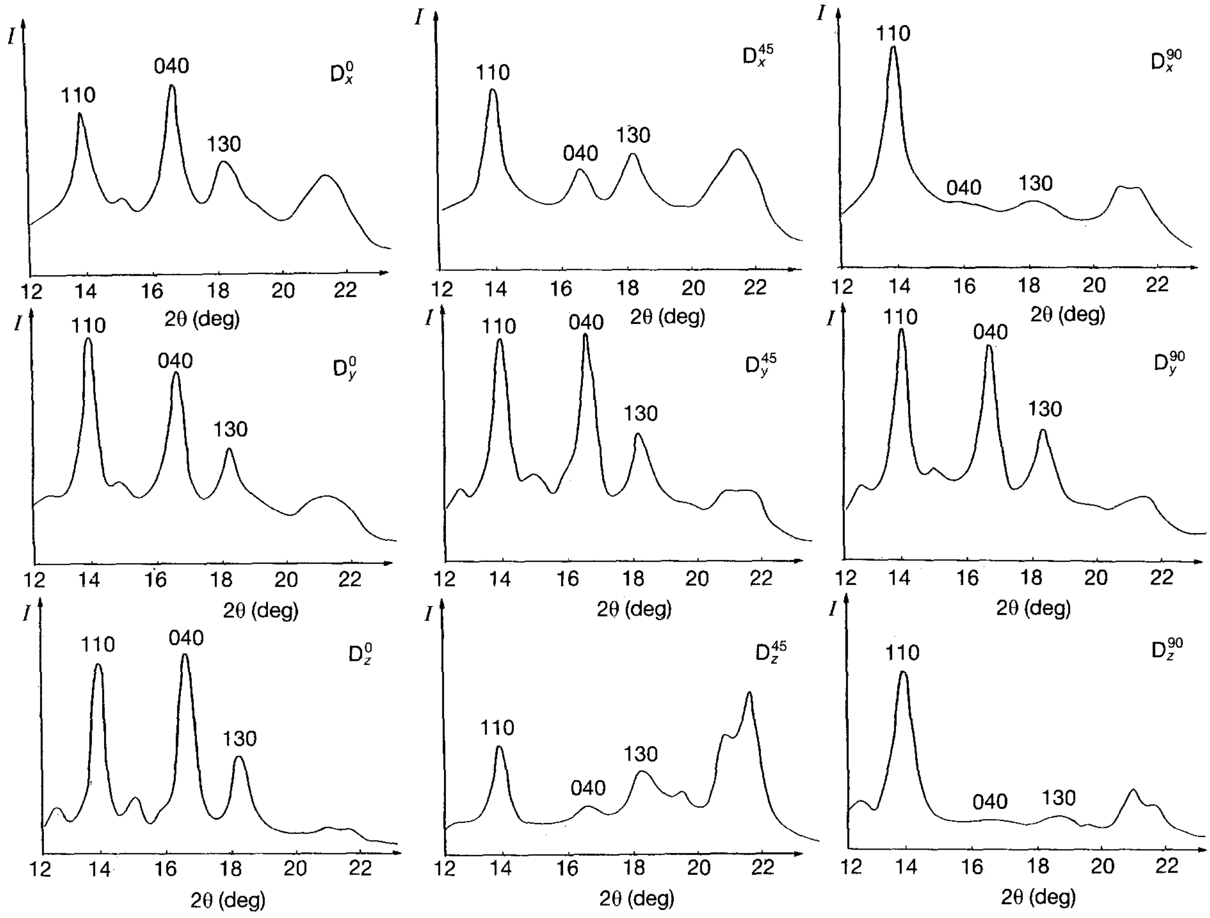

Figure 3 Diffraction patterns for pure injected iPP.

have a monoclinic unit cell; *l* corresponds to the vector *c* which is parallel to the chain axis.

Since the variations of intensity are similar to the variations reported by Mencik and Fitchum [6], we conclude that either *a* or *c* are parallel to the injection direction in the sheets: the *c* orientation is indicated by the strong (1 1 0) and (0 4 0) reflexions on D_x^0 and D_z^0; the *a* orientation is indicated by the strong (1 1 0) reflexion on D_x^{90} and D_z^{90}.

Though the heights of the (1 1 0) peaks are similar on diffractograms D_x^0 and D_x^{90}, transverse isotropy implies that more atomic layers lead to diffraction on D_x^0 than on D_x^{90}. Thus the *c* orientation is the preferred orientation. It corresponds to the orientation of polymer chains along the injection direction.

This is confirmed by small angle results: Fig. 4 shows these results on D_z^0 and D_z^{90}. The position of the maximum corresponds to a crystalline long period of about 15 nm. The transmitted beam is nearly extinguished on the D_z^0 pattern. This indicates that lamellae [7] are preferentially oriented along the injection direction with their surfaces perpendicular to this direction. Since chains have a perpendicular orientation in folded chain lamellae [7], the latter observation is consistent with results obtained from WAXS measurements.

In order to check if anisotropy at a scale of about 1 nm and about 10 nm observed by WAXS and SAXS, respectively, is related to the injection conditions, SEM observations were performed.

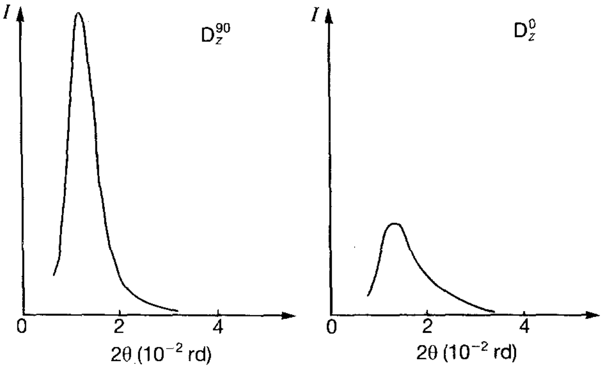

Figure 4 Small angle results for pure injected iPP.

Fig. 5 shows surfaces after etching observed at (i) 0.5 mm and (ii) 1 mm from one edge of the sheet. Fig. 5b shows structures which are oriented along the injection direction. In contrast, Fig. 5a shows radial structures corresponding to usual spherulites. For our samples of 2 mm thickness, the former case corresponds to regions in the sheet where the shear rate was high during the filling of the mould, while the latter case corresponds to regions where the shear rate was zero for reasons of symmetry. Thus, chains, and therefore crystallites, should not be oriented in the central region of the sheets.

X-ray measurements were also used to investigate crystalline orientation of PA12. Fig. 6 shows

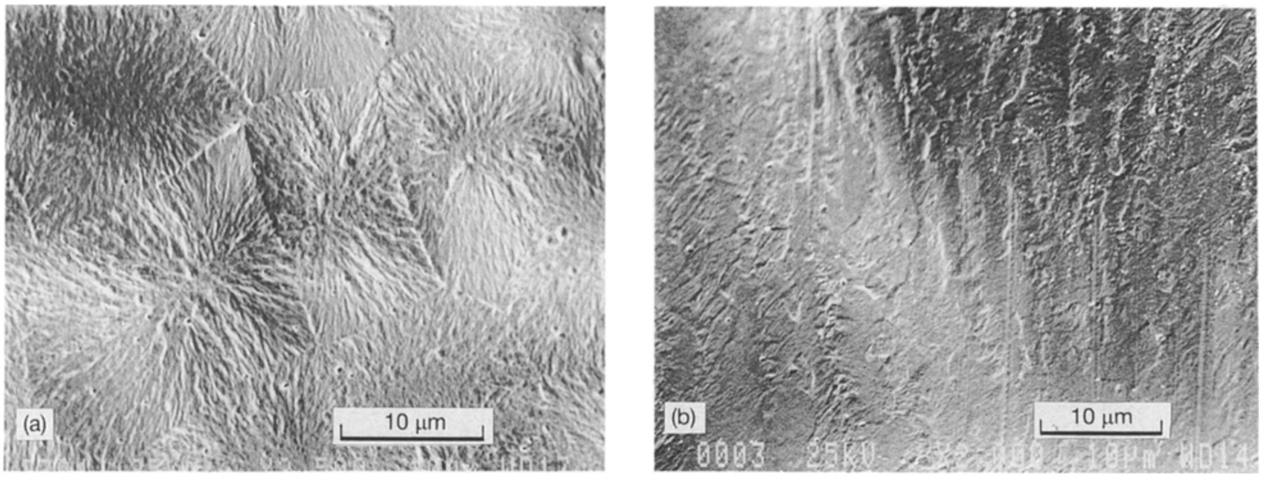

Figure 5 Micrographs of iPP after etching: (a) 1 mm from one edge of the sheet; (b) 0.5 mm from one edge of the sheet.

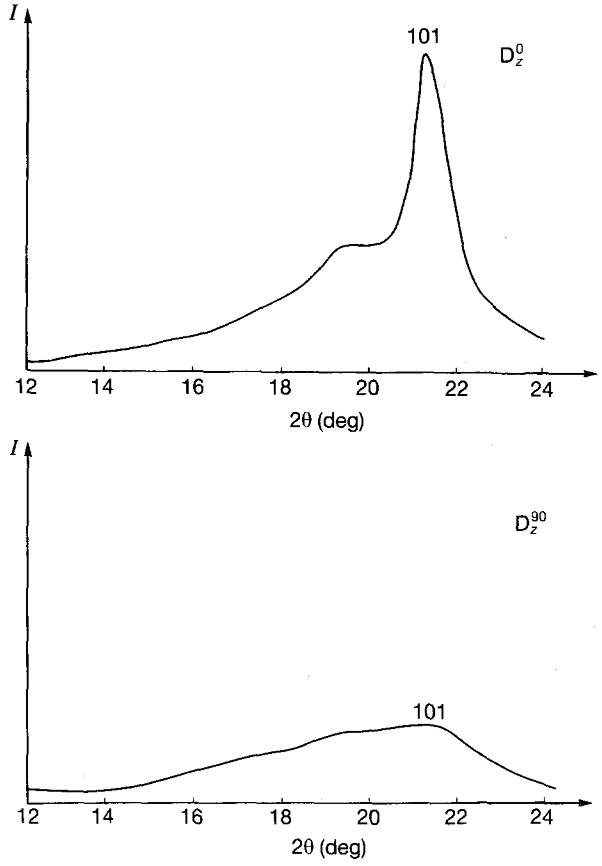

Figure 6 Diffraction patterns for pure injected PA12.

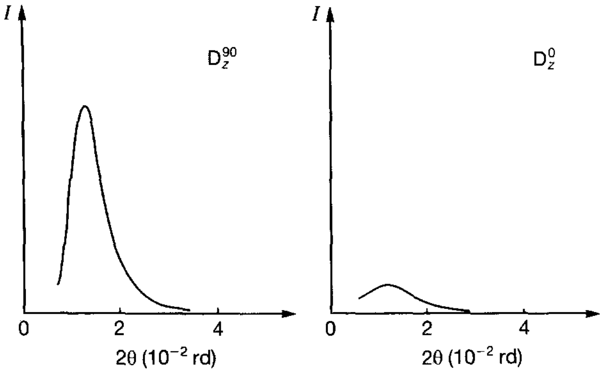

Figure 7 Small angle results for pure injected PA12.

diffraction patterns D_z^0 and D_z^{90} for an incident beam oriented along the z axis.

The main diffraction peak corresponds to (1 0 1) layers of the γ form which are parallel to chain axis [8, 9]. The peak (1 0 1) is about 10 times higher on D_z^0 than on D_z^{90}. This result indicates that most of the (1 0 1) layers are parallel to the y axis, which is the injection direction. Furthermore, from SAXS experiments (Fig. 7) it is shown that most of the lamellae are perpendicular to the y axis. Thus, we can conclude that the chains are mostly parallel to the injection direction. The same types of observations were made on all the samples studied here, leading to similar conclusions. Thus the anisotropy in the mechanical behaviour (part 2) could be partly due to the anisotropy in chain orientation, which is a result of the material processing.

4.2. Morphology of homopolymer domains

4.2.1. Dynamic mechanical behaviour

Fig. 8 shows data for pure homopolymers: modulus and internal friction G''/G' at a frequency of 0.1 Hz are plotted on the same figure. PA12 shows two principal relaxations called α and γ which are due to molecular motions in the amorphous phase [4]. iPP shows two relaxations α and β; β is associated with the glass transition of the amorphous phase [8, 10]. α is related to the local motion of segmented parts of molecules in the crystalline phase. Three sets of mechanical models were used for calculation of the complex shear modulus of blends.

The Voigt limit, which corresponds to the ideal case where the strain is homogeneous in the composite material, so that the modulus of the composite G_c is obtained by a mixing law of the moduli of each phase ($G1$ and $G2$), $G_c = G_1 V + G_2(1 - V)$, where V is the volume fraction of phase 1.

The Reuss limit, which corresponds to the ideal case where the stress is homogeneous in the composite. Thus $(G_c)^{-1} = (G_1)^{-1}\ V + (G_2)^{-1}(1 - V)$.

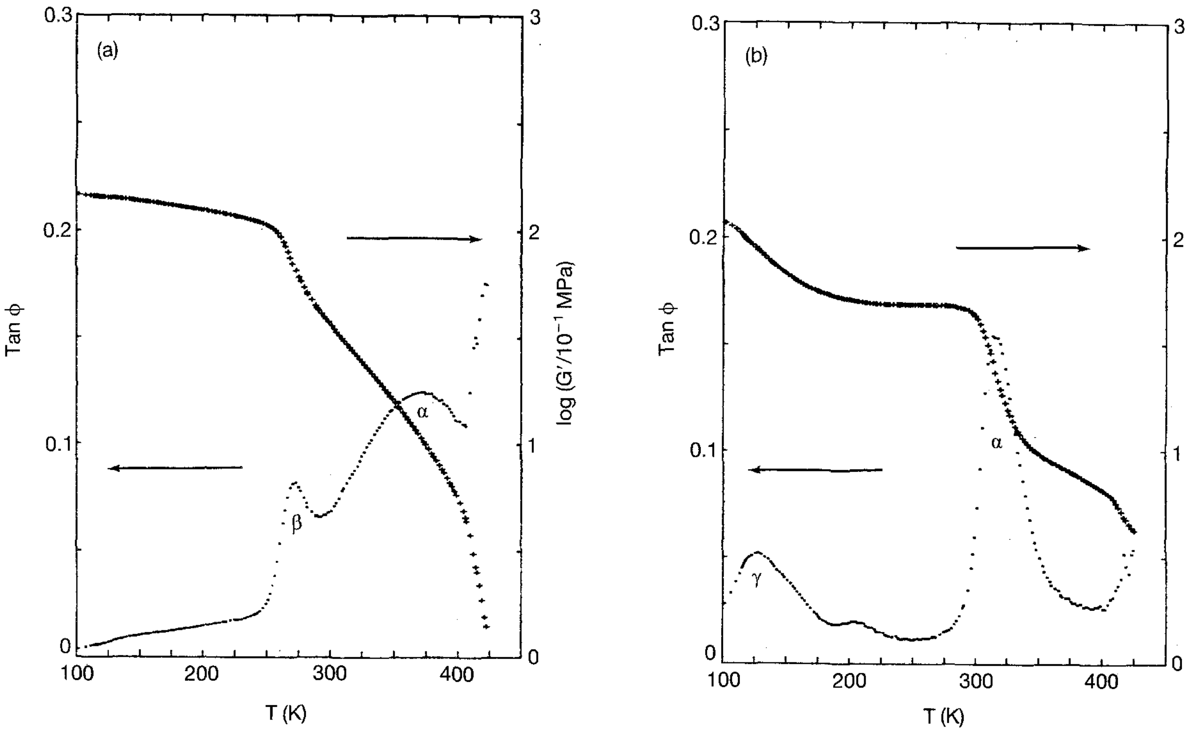

Figure 8 Dynamic mechanical behaviour of homopolymers (a) iPP and (b) PA12.

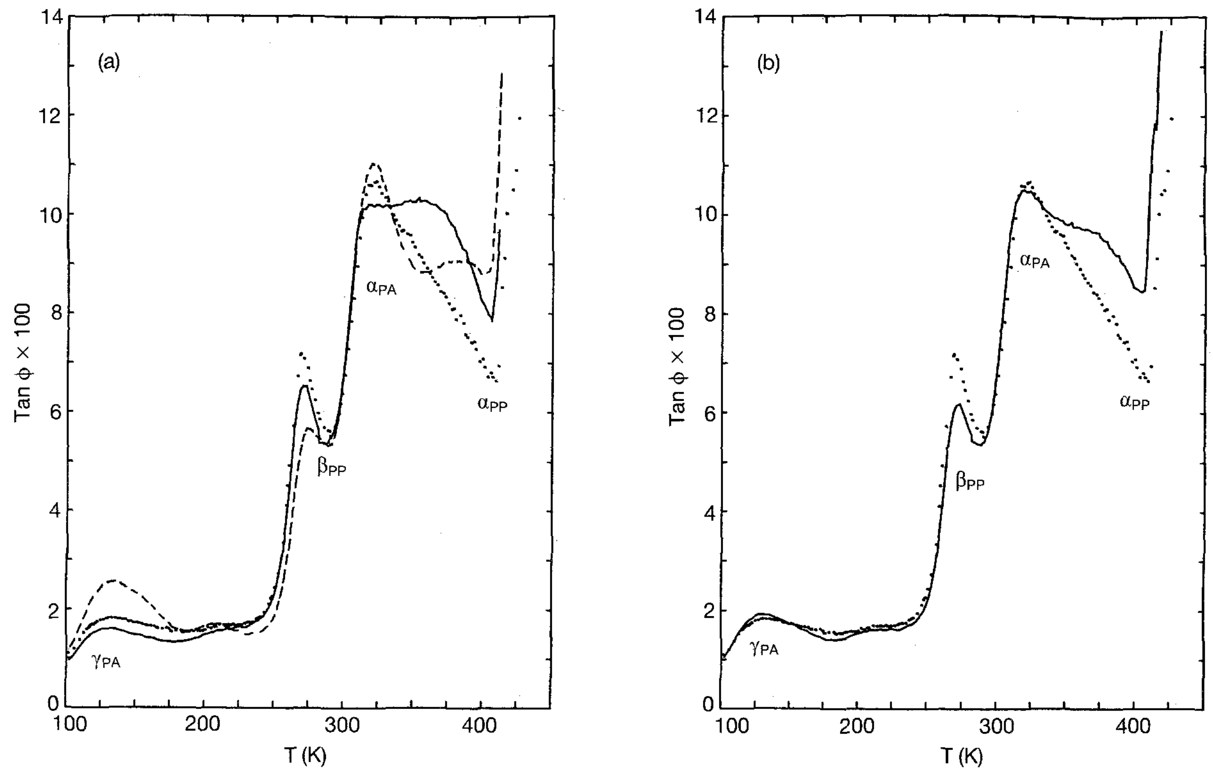

Figure 9 Comparison between experimental and calculated data for blend D2. (a) . . . Experimental; - - - - - Reuss limit; ——— Voigt limit. (b) . . . Experimental; —— Kerner model.

The Kerner–Dickie equation [11, 12].

G_i^* is the complex shear modulus of the inclusions and G_m^* is the complex shear modulus of the matrix. These moduli are supposed to be isotropic and homogeneous in each homopolymer domain. It is noteworthy that the Voigt and Reuss limits correspond to the upper and lower limits for the behaviour of the real blends. The results obtained by any other model always lie between these limits. Experimental data for blends are nearly independent of TC content. Thus, predicted data are calculated for PA12/iPP composites without TC contribution. Although the sheets are strongly oriented by the injection process, data are quite independent of the orientation of samples when shear moduli are considered. Thus, the hypothesis of isotropy of the components is well-adapted. Fig. 9

shows a comparison between experimental and calculated data for the D2 blend. The Kerner equation [11] modified by Dickie [12] (Fig. 9b) with iPP as a matrix provides the best fit [13]. This leads us to conclude that PA12 forms inclusions in an iPP matrix. Despite the good fit, there is a difference between calculated and experimental data in the range of the α relaxation of iPP.

Fig. 10 shows a comparison between experimental and calculated data for the I blend. In this case, the Voigt limit provides the best fit. Since the Kerner model with PA12 as a matrix is not well adapted, we conclude that iPP does not form inclusions in a PA12 matrix. The fact that the Voigt model agrees reasonably with our data suggests a co-continuous morphology for this blend. If the homopolymer domains are

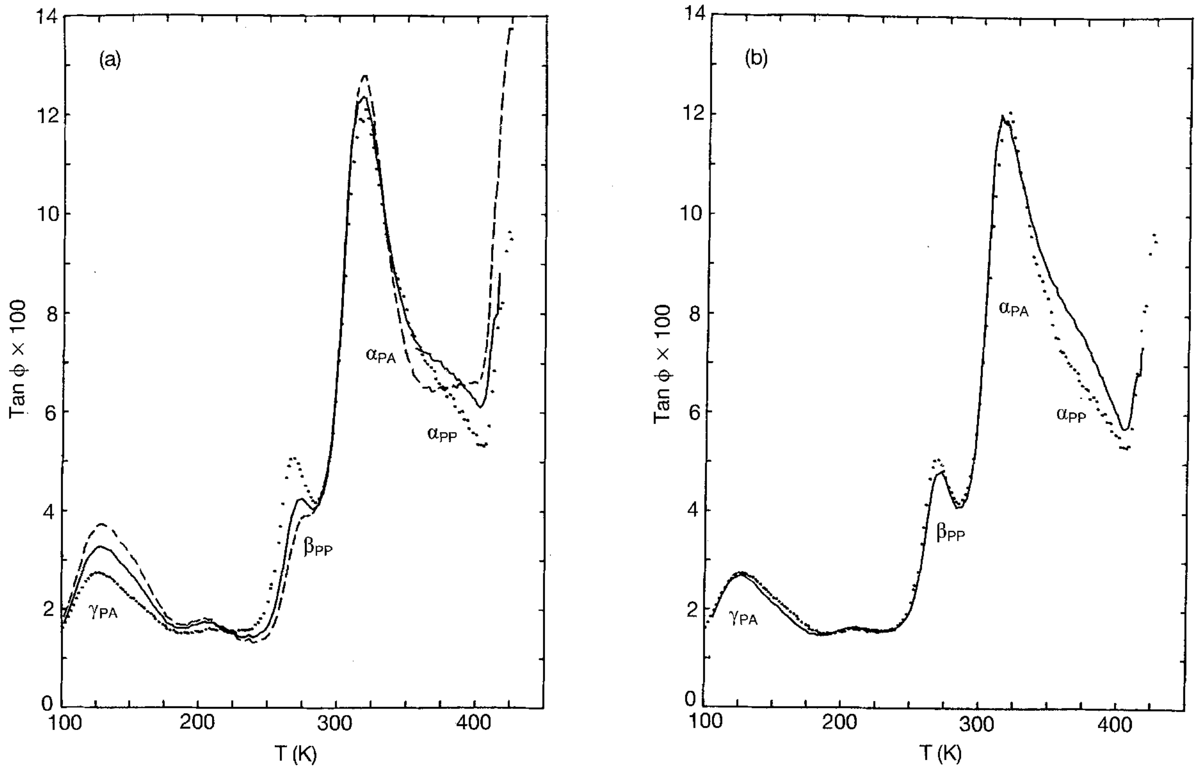

Figure 10 Comparison between experimental and calculated data for blend 1. (a) . . . Experimental; - - - - - Reuss limit; ——— Kerner model. (b) . . . Experimental; —— Voigt limit.

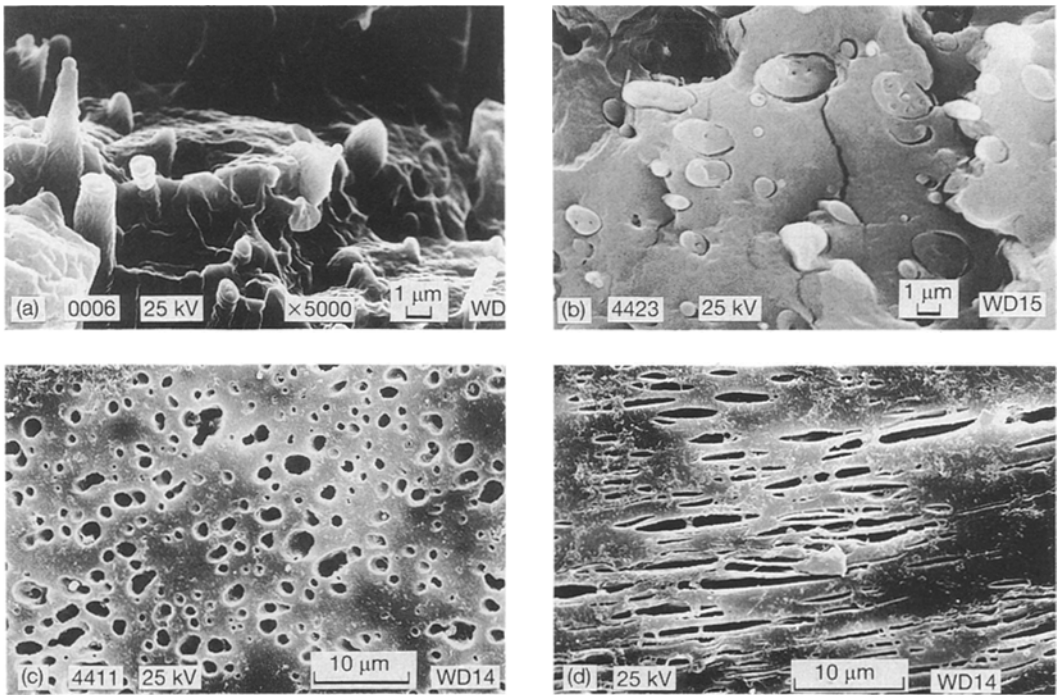

Figure 11 SEM micrographies of blend D2: (a) fracture surface along the injection direction; (b) fracture surface perpendicular to the injection; (c) surface cut parallel to the surface of the sheet, 1 mm from one edge (core); (d) surface cut parallel to the surface of the sheet, close to the surface.

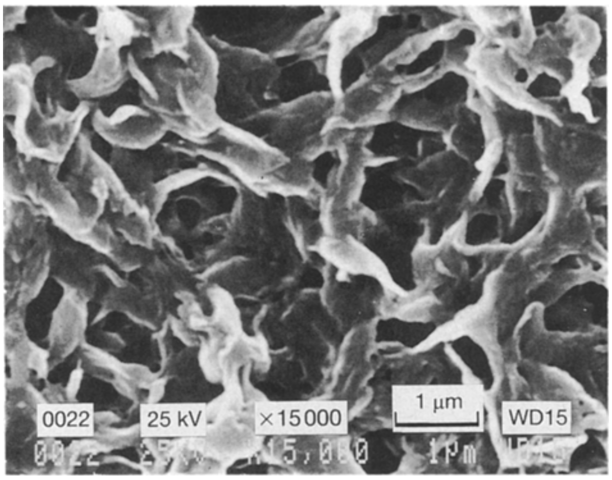

Figure 12 SEM micrography of blend I.

interpenetrated, strain is nearly homogeneous and the moduli follow a mixing law.

Lastly, we can remark that the range of the α relaxation of iPP, as in direct blends, is not well fitted by the model. Since this observation was made for the direct and inverse blends, we conclude that in all blends the crystalline phase of iPP is modified. The presence of PA12 and TC could explain such a modification. It is well known that polyamides are nucleating agents for iPP [14, 15].

4.2.2. SEM

Fig. 11 shows micrographs of the D2 blend obtained on fractured surfaces [(a) and (b)] and on surfaces obtained by cutting and extracting samples [(c) and (d)]. Fig. 11a corresponds to a fracture plane parallel to the injection direction. Fig. 11b corresponds to a plane perpendicular to this direction. Inclusions of about 2 µm are clearly observed. These inclusions are elongated along the injection direction. In the case of the blend D10, the size of inclusions is about 0.5 µm. Thus, TC has an important effect on particle size.

Fig. 11c corresponds to a plane parallel to the sheet at the core of the sheet. Fig. 11d corresponds to a plane parallel to the sheet in a region close to the plate surface (< 0.1 mm). PA12 which is extracted appears as black holes. This is consistent with our conclusion, based on dynamic mechanical measurements, that direct blends consist of PA12 inclusions in an iPP matrix. Since these inclusions are symmetrical in the middle of the sheet, their elongation seems to be due to the shear rate during the filling of the mould, as is the crystalline orientation.

Fig. 12 shows a micrograph of the blend I. The complex morphology shown here is in agreement with previous conclusions from dynamic mechanical measurements, i.e. that the two polymers form interpenetrated domains.

5. Relationships between homopolymer morphology and mechanical properties

For blends D, the elongation of particles is a new element which explains the mechanical anisotropy. The Grifith theory permits us to link the stress concentration around an elliptical crack to the curvature radius [16]. Since the curvature radius is high on the extremities of elongated inclusions, crack propagation is easier for a tensile force applied along a direction perpendicular to the elongation. Thus, crystalline orientation and particle elongations are two factors which can lead to a mechanical anisotropy.

For pure polypropylene only the first factor has to be considered. This probably explains why mechanical anisotropy is lower than for blends.

The high brittleness of the inverse blend can be attributed to its particular morphology. Since homopolymer domains are continuous, a single crack can propagate throughout the blend and lead to its break.

6. Conclusion

By X-ray techniques we have characterized an orientation of the crystalline phases which occurs in the samples as a result of the injection-moulding preparation technique. The mechanical spectrometry and scanning electron microscopy results have been combined to show the specific geometrical arrangement of the homopolymer regions, as well as the changes that occur in these regions as they are mixed. The microstructural information thus obtained permit us to interpret the main features of the large deformation response of the blends, such as its anisotropic nature. We have shown that the preparation technique, including compounding and injection moulding, modifies several features of the final material. Using X-ray scattering techniques we have characterized the orientation of the crystalline phases which occur during the injection process, in homopolymers and in blends. Using mechanical spectrometry and scanning electron microscopy we have determined the geometrical and topological arrangements of homopolymer domains. In both cases, the shear stress field which is induced in the mould by the injection conditions is responsible for the anisotropy in the final material. Thus, for blends with a predominance of iPP, domains of PA12 are ellipsoidal inclusions with their long axis along the injection direction. Moreover, for blends with a predominance of PA12 and for the preparation conditions used for this work, both types of domains, namely PA12 and iPP, are continuous in the material.

On the other hand, the additive TC is shown to play a major role (i) on the final size of inclusions and (ii) on the ultimate mechanical properties.

Acknowledgement

We gratefully acknowledge Dr B. Lotz (Institut Charles Sadron, CNRS, Strasbourg) for helpful discussions.

References

1. D. R. NORTON and A. KELLER, *Polymer* **26** (1985) 704.
2. J. Y. CAVAILLÉ, C. JOURDAN and J. PEREZ, *Makromol. Chem.* **16** (1988) 341.
3. R. M. CHRISTENSEN, "Mechanics of Composite Materials" (Wiley, 1979).

4. J. VARLET, J. Y. CAVAILLÉ, J. PEREZ and G. P. JOHARI, *J. Polym. Sci. Polym. Phys.* **28** (1990) 2691.
5. G. NATTA and P. CORRADINI, *Nuovo Cimento* **15** (1960) 40.
6. Z. MENCIK and D. R. FITCHUM, *J. Polym. Sci. Polym. Phys.* **11** (1973) 973,
7. B. WUNDERLICH, "Macromolecular Physics" (Academic Press, 1973).
8. R. BOYER, *J. Polym. Sci. Polym. Part C* **50** (1975) 189.
9. G. COJAZZI, A. FICHERA, C. GARBUGLIO, V. MALTA and R. ZANNETTI, *Makromol. Chem.* **168** (1973) 289.
10. C. JOURDAN, PhD thesis, INSA Lyon, Lyon, France (1987).
11. E. H. KERNER, *Proc. Phys. Soc.* **B69** (1956) 808.
12. R. A. DICKIE, *J. Appl. Polym. Sci.* **17** (1973) 45.
13. J. VARLET, PhD thesis, INSA Lyon, Lyon, France (1990).
14. D. CAMPBELL and M. M. QUAYYUM, *J. Polym. Sci. Polym. Phys.* **18** (1980) 83.
15. B. LOTZ and J. C. WITTMANN, *ibid.* **24** (1986) 1559.
16. W. KURZ, J. P. MECIER and G. ZAMBELLI, "Introduction à la Science des Matériaux" (Presses polytechniques romandes, 1987).

Received 28 January
and accepted 29 October 1992